THE ASTROPHYSICAL JOURNAL, 355:357–372, 1990 May 20

THE PHYSICAL AND INFRARED SPECTRAL PROPERTIES OF CO_2 IN ASTROPHYSICAL ICE ANALOGS

S. A. SANDFORD AND L. J. ALLAMANDOLA
NASA/Ames Research Center
Received 1989 September 8; accepted 1989 November 29

ABSTRACT

Both laboratory measurements and theory indicate that CO_2 should be a common component in interstellar ices. We show that the exact band position, width, and profile of the solid-state $^{12}CO_2$ infrared bands near 3705, 3600, 2340, and 660 cm^{-1} (2.70, 2.78, 4.27, and 15.2 μm) and the $^{13}CO_2$ band near 2280 cm^{-1} (4.39 μm) are dependent on the matrix in which the CO_2 is frozen. Measurements of these bands in astronomical spectra can be used to determine column densities of solid-state CO_2 and provide important information on the physical conditions present in the ice grains of which the CO_2 is a part. Depending on the composition of the ice, the CO_2 asymmetric stretching band was observed to vary from 2328.7 to 2346.0 cm^{-1} and have full widths at half-maxima (FWHMs) ranging from 4.7 to 29.9 cm^{-1}. The other CO_2 bands showed similar variations. Both position and width are also concentration dependent. Absorption coefficients were determined for the five CO_2 bands. These were found to be temperature independent for CO_2 in CO and CO_2 matrices but varied slightly with temperature for CO_2 in H_2O-rich ices. For all five bands this variation was found to be less than 15% from 10 to 150 K, the temperature at which H_2O ice sublimes.

A number of parameters associated with the physical behavior of CO_2 in CO_2- and H_2O-rich ices were also determined. The CO_2-CO_2 surface binding energy in pure CO_2 ices is found to be $(\Delta H_s/k) = 2690 \pm 50$ K. CO_2-H_2O and CO-H_2O surface binding energies were determined to be $(\Delta H_s/k) = 2860 \pm 200$ K and 1740 ± 100 K, respectively. Under our experimental conditions, CO_2 condenses in measurable quantities into H_2O-rich ices at temperatures up to 100 K, only slightly higher than the temperature at which pure CO_2 condenses. Once frozen into an H_2O-rich ice, the subsequent loss of CO_2 upon warming is highly dependent on concentration. For ices with $H_2O/CO_2 > 20$, the CO_2 is physically trapped within the H_2O lattice, and little CO_2 is lost until the sublimation temperature of the H_2O matrix is reached. In contrast, in ices having $H_2O/CO_2 < 5$, the CO_2 remains only to temperatures of about 90 K. Above this point the CO_2 readily diffuses out of the H_2O matrix. These results suggest that two different forms of H_2O lattice are produced. The implications of these data for cometary models and our understanding of cometary formation are considered.

Subject headings: infrared: spectra — interstellar: grains — interstellar: molecules — laboratory spectra — line identifications — molecular processes

I. INTRODUCTION

During the past 15 years, great strides have been made in our understanding of the composition of interstellar ice grains and the roles they play in interstellar chemistry. These gains have been made possible by the substantial advances in astronomical infrared spectroscopic techniques combined with the availability of spectra of realistic laboratory analogs. Interstellar ice band assignments that have been made in this way include H_2O, CH_3OH, CO, H_2CO, and HCO (see Tielens and Allamandola 1987; Allamandola and Sandford 1988 for recent reviews). An important component that is quite likely to be present in interstellar ices, but which is currently not detectable, is CO_2. Virtually all laboratory experiments involving energetic processing (UV irradiation or particle bombardment) of interstellar ice analogs readily produce entrapped CO_2 (see, for example, Moore *et al.* 1983; d'Hendecourt *et al.* 1986; Allamandola, Sandford, and Valero 1988; Sandford *et al.* 1988). Because of the efficient production of CO_2 in these experiments, the growth of the CO_2 stretching band near 2340 cm^{-1} (4.274 μm) is one of the most striking aspects of the spectral evolution of the mid-infrared region. The CO_2 produced in these experiments contains an appreciable fraction of the carbon present in the ices (Sandford *et al.* 1988). In addition, theoretical calculations predict that CO_2 should be present on interstellar grain mantles in interstellar clouds (Tielens and Hagen 1982; d'Hendecourt, Allamandola, and Greenberg 1985). In view of these considerations, it seem reasonable to assume that CO_2 is an abundant component of interstellar ice grains, that it can carry a significant fraction of interstellar carbon in molecular clouds, and that its measurement will provide an important tracer of cloud chemistry.

Unfortunately, the search for interstellar CO_2 requires spaceborne instrumentation. Since CO_2 does not have a permanent dipole moment, it does not have a pure rotational spectrum and is therefore undetectable at radio frequencies. CO_2 produces five spectral bands in the mid-infrared, but telluric CO_2 makes astronomical detection of this molecule impossible with ground and airborne telescopes. One of the original purposes of this paper was to provide an infrared spectral data base of ice analogs necessary to guide the search for solid interstellar CO_2 and to provide the information needed to interpret the interstellar CO_2 bands once found. After submission of the original version of this paper, we received a preprint by d'Hendecourt and Jourdain de Muizon (1989) in which they report the detection of a band near 13.5 μm in the *IRAS* LRS data of several objects. They interpret this band in terms of the ν_2 bending mode of CO_2. This exciting discovery only serves to emphasize the importance of the laboratory data presented here.

The infrared spectra of pure CO_2 films (Osberg and Hornig 1952; Yamada and Person 1964; Wood and Roux 1982; Warren 1986; Falk and Seto 1986; Falk 1987) and CO_2 in rare gas and nonastrophysical matrices (Fredin, Nelander, and Ribbegard 1974; Guasti, Schettino, and Brigot 1978; Irvine, Mathieson, and Pullin 1982*a*, *b*; Tso and Lee 1985*a*, *b*) have been investigated in detail, but the study of the spectroscopic properties of CO_2 in astrophysically relevant mixed molecular ices has only just begun (Langenscheidt, Patnaik, and Roessler 1990). The results reported here demonstrate that laboratory-derived CO_2 integrated band strengths can confidently be used to determine the column density of CO_2 frozen in interstellar grains, and that the solid CO_2 band profiles and positions can be used to provide important insight into the composition and themal history of interstellar ices.

CO_2 is also thought to be important in determining some of the properties of comets. CO_2 was detected in the coma of comet Halley (Combes *et al.* 1986, 1988; Krankowsky *et al.* 1986; Feldman *et al.* 1986) and is believed to be a common component of most comets (Delsemme 1982). There may be a connection between interstellar and cometary CO_2, since comets may have formed by the accretion of preexisting interstellar ice-bearing grains or through the accretion of grains formed by condensation of protosolar gases at large solar distances (Donn and Rahe 1982; Greenberg 1982). The amount of CO_2 in comets as inferred from the coma measurements is typically on the order of a few percent of the H_2O, a number similar to the amount typically produced in laboratory ice irradiation studies.

Since CO_2 in comets may occur in pockets of pure CO_2 or be intimately mixed in an H_2O lattice prior to its ejection into the gas phase, knowledge of the condensation/vaporization properties of CO_2 and H_2O:CO_2 ices is essential in understanding cometary behavior. While the condensation, vaporization, and diffusion properties of pure solids such as CO_2 and H_2O are individually well known (see Smith 1929; Hobbs 1974, and references therein), detailed studies of the vaporization and trapping properties of mixed molecular ices have only recently become available (Bar-Nun *et al.* 1985, 1987; Laufer, Kochavi, and Bar-Nun 1987; Schmitt and Klinger 1987; Sandford and Allamandola 1988; Hudson and Donn 1988). With the exception of the work reported by Hudson and Donn (1988), the physical behavior of CO_2 in H_2O in astrophysically relevant concentrations has not been described. In the experiments reported here, we show that the vaporization behavior of CO_2 in H_2O ices is unique and cannot be predicted on the basis of previous knowledge of other gases trapped in H_2O.

In this paper we report the results of measurements of the infrared spectroscopic and condensation-vaporization properties of CO_2 in pure and mixed ices. In the interest of clarity, after describing our experimental techniques, the results are presented in two major sections. The first section discusses the spectral properties of CO_2-bearing ices. These include the matrix and temperature dependence of the peak positions, full widths at half-maxima (FWHMs), band profiles, and integrated absorbances (band strengths) of the CO_2 fundamentals near 2340, 2280, and 660 cm^{-1} (4.27, 4.39, and 15.2 μm) and the CO_2 combination bands near 3705 and 3600 cm^{-1} (2.70 and 2.78 μm). It is shown that good quality, moderate- to high-resolution spectra of the interstellar CO_2 feature can provide important information about the composition, temperature, and thermal history of interstellar and precometary ices containing CO_2. In the second section, a series of experiments on the temperature and concentration dependence of the condensation and vaporization properties of CO_2 in pure and H_2O-rich ices is presented. The astrophysical implications of these properties, including binding energies, "sticking" coefficients, and related parameters, are then discussed.

II. EXPERIMENTAL PROCEDURES

Only a brief summary of the laboratory procedures used is given here. For a more detailed description see Allamandola, Sandford, and Valero (1988).

All the gas mixtures were prepared in a greaseless, glass vacuum system calibrated to allow for careful control of the concentrations of species mixed in each sample bulb. H_2O and CH_3OH (initially 99.5% pure) were thoroughly degassed at room temperature and then further purified by three freeze-thaw cycles under vacuum. CO, CO_2, and O_2 (purity greater than 99.5%) were taken directly from lecture bottles and used without further purification.

After allowing ample time for complete mixing, samples were slowly condensed onto a CsI window suspended in a vacuum chamber. Depositions were made at a pressure of about 3×10^{-8} mbar. Infrared spectra show that under these conditions a mixed molecular amorphous ice is formed, not a crystalline or clathrate structure. The flow of gas onto the CsI window was regulated by a microflowmeter, and samples were typically deposited in the infrared beam at a rate of 6×10^{-6} moles hr^{-1} (about 2 μm hr^{-1}). Sample deposition typically took 5 minutes. The window temperature was controlled by a closed cycle helium refrigerator. Using a resistive heater, the temperature of the CsI window could be maintained at any point between 10 and 280 K. The temperature was measured with an absolute accuracy of ± 2 K and a relative accuracy of ± 0.2 K with an Fe-Au/Chromel thermocouple placed in a small hole inside the window mounting. The resistive heater could be controlled in such a manner as to allow for sample warm-up or cool-down at predetermined rates. All the warm-ups described in this paper were done at a rate of 2 K per minute. The CsI window is rotatable and besides facing the deposition port, it can be rotated to face the beam axis of a Fourier transform infrared spectrometer.

Infrared transmission spectra were measured from 4000 to 400 cm^{-1} (2.5–25 μm) using a Nicolet 740 Fourier transform spectrometer. The resolution was 1 cm^{-1} with a frequency accuracy of ± 0.2 cm^{-1}. Spectra taken during warm-up experiments were made while the temperature was held constant at the warm-up temperature.

III. RESULTS AND DISCUSSION

a) The Spectral Properties of CO_2-bearing Ices

CO_2 has five active bands in the mid-infrared (4000–400 cm^{-1}, 2.5–25 μm) (Fig. 1). In this section, the spectral properties of each of these bands will be discussed individually. Properties examined include peak position, full width at half-maximum (FWHM), band shape, and absorption strength. The dependence of these quantities on matrix composition and temperature is also examined.

Before presenting the results in detail, it is appropriate to briefly review why these properties can vary as a function of ice composition and temperature. The fundamental vibrations of a molecule suspended in a solid matrix may be blueshifted or redshifted from their gas phase frequencies due to chemical or

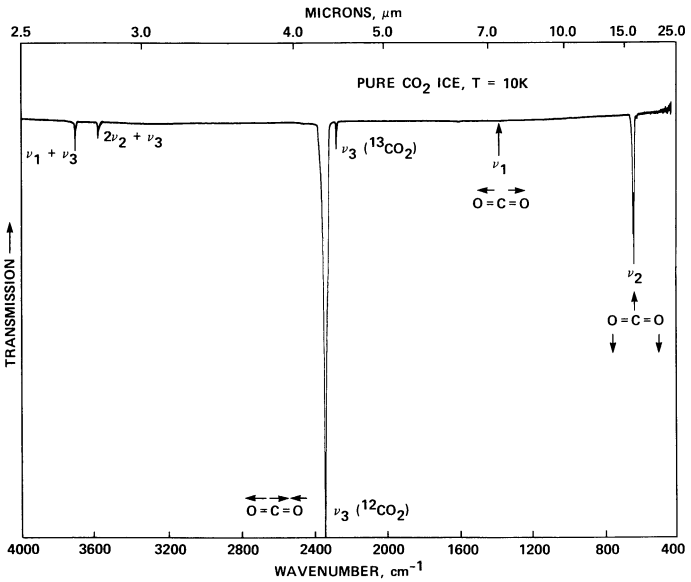

FIG. 1.—Spectrum of an amorphous pure CO_2 ice deposited and held at 10 K. Each of the five CO_2 bands discussed in this paper are labeled, and the associated vibration is schematically identified.

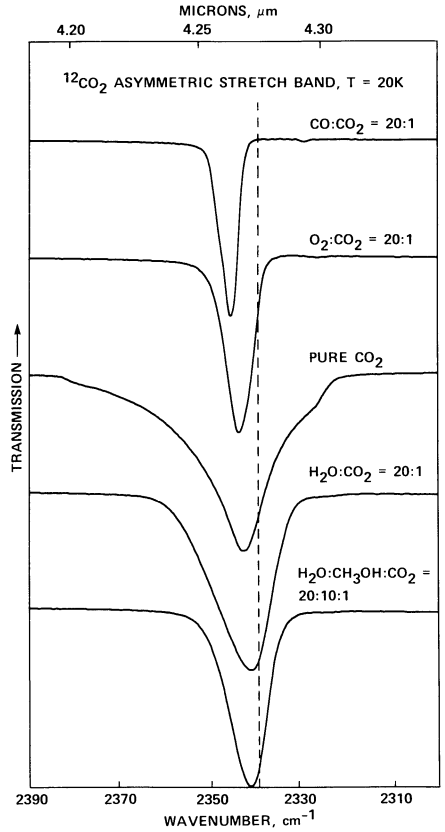

FIG. 2.—The asymmetric stretching vibration (ν_3) of $^{12}CO_2$ in different matrices at 20 K. All the ices were deposited at 10 K and warmed to 20 K. A dashed line is given at 2340 cm^{-1} for reference. Note that the weak $^{18}O^{12}C^{16}O$ band near 2330 cm^{-1} is just discernible in the upper two spectra.

physical interactions with the surrounding matrix molecules. When species are deposited at temperatures much lower than their melting point, an amorphous, rather than crystalline structure is produced. Under these conditions, each individual molecule has insufficient energy to reorient itself into more energetically favorable positions, and a highly disordered solid is produced. Thus, impurities in an amorphous ice experience a wider range of molecular site geometries and environments than a crystalline solid. This produces Gaussian-like infrared band profiles which are broader than those of crystalline solids. Upon warming, the molecules in these ices rearrange into more energetically favorable orientations, and somewhat more ordered amorphous structures are produced. This process, called annealing, usually produces sharper bands because the range of different environments is reduced.

i) *Band Positions, Widths, and Profiles as a Function of Temperature and Matrix Composition*

1. *The $^{12}CO_2$ asymmetric stretching fundamental (ν_3).*—The strongest CO_2 infrared band is produced by C=O asymmetric stretching vibrations and falls near 2340 cm^{-1} (4.27 μm) (Fig. 1). Figure 2 illustrates the position, width, and profile dependence of this band on matrix material. A summary of band positions and widths is given in Table 1.

Typically, this band is redshifted by 2–8 cm^{-1} from the gas phase value (2348 cm^{-1}). This suggests that in these solids (1) the trapping site is generally slightly larger than the CO_2 molecule, since more cramped sites produce blueshifts, or (2) a weak chemical complex is formed in which some of the bonding electrons of the CO_2 are delocalized, resulting in a slightly weaker C=O bond. Deciding between these two alternatives would require additional experiments beyond the scope of this work. The amount of the shift is matrix dependent. For example, CO_2 in CO undergoes a smaller shift than CO_2 in the other matrices examined.

Much more striking matrix-dependent differences are seen in the bandwidths and profiles. CO_2 frozen in H_2O-rich ices produces a relatively broad band (10–20 cm^{-1}), while CO_2 frozen in O_2 and CO matrices yields narrower bands (<7 cm^{-1}).

The position and width of the CO_2 asymmetric stretch band is temperature dependent. Figure 3 illustrates this band as a function of temperature. In all cases, the ice was deposited at 10 K and warmed at a rate of 2 K per minute to the temperatures at which the spectra were measured. Band positions and widths for these experiments are also listed in Table 1. In general, the bands decrease in width as the temperature is increased. CO_2 in O_2 matrices provides the only exception to this behavior. Band positions often show systematic temperature-dependent changes as well. For instance, in H_2O the band peak steadily shifts to lower frequencies as the temperature increases. For H_2O:CO_2 = 20:1, this shift is about 2 cm^{-1} over the entire 10–150 K range.

While the majority of the ices show the general behavior mentioned above, several deserve special attention. The CO_2 band produced by pure CO_2 ice is noteworthy in several respects. First, it shows a wing on the high-frequency side of the band that persists over most of the ice's thermal stability range. Second, at 10 K it has a strong shoulder on the low-frequency side of the main band. This band rapidly decreases in strength as the ice is warmed from 10 to 20 K. Apart from this shoulder and a 1 cm^{-1} difference in band position, our results for pure CO_2 ice are in agreement with the properties of amorphous CO_2 reported by Falk (1987). Falk deposited his ices using gas pulses, whereas ours were prepared by contin-

TABLE 1

POSITION AND WIDTH OF THE $^{12}CO_2$ AND $^{13}CO_2$ ASYMMETRIC STRETCHING MODE AND BENDING MODE BANDS IN VARIOUS ICE MIXTURES

Ice Composition	$^{12}CO_2$ Stretch Peak and FWHM[a] (cm^{-1})	$^{13}CO_2$ Stretch Peak and FWHM[a] (cm^{-1})	$^{12}CO_2$ Bend Peak and FWHM[a] (cm^{-1})
CO_2			
(10 K).....	2342.6 (16.5)[b]	2282.6 (3.1)	659.5, 654.4 (10)[c]
(20 K).....	2342.7 (16.5)	2282.7 (2.7)	659.5, 654.4 (10)[c]
(50 K).....	2343.3 (13.9)	2282.5 (2.3)	659.5, 654.6 (3.1, 2.4)
(80 K).....	2343.3 (4.7)	2282.4 (1.8)	659.6, 654.7 (1.4, 1.2)
$CO:CO_2 = 20:1$			
(10 K).....	2346.0 (4.9)	2281.0 (1.6)	659.1 (3.4)
(20 K).....	2346.0 (4.7)	2280.9 (1.4)	659.0 (3.0)
$O_2:CO_2 = 20:1$			
(10 K).....	2342.4 (6.2)	2277.5 (3.7)	662.4 (4.1)
(20 K).....	2344.0 (6.9)	2278.5 (3.8)	662.4 (5.0)
$H_2O:CO_2 = 50:1$			
(10 K).....	2341.7 (11.0)	2277.5 (7.8)	653.3 (26.6)
(50 K).....	2340.6 (9.3)	2276.0 (6.5)	654.5 (20.0)
(100 K).....	2339.9 (7.5)	2275.5 (5.1)	654.6 (17.4)
(150 K).....	2339.9 (6.7)	2275.2 (4.5)	654.7 (17.0)
$H_2O:CO_2 = 20:1$			
(10 K).....	2341.5 (14.3)	2277.2 (8.3)	653.4 (25.2)
(20 K).....	2341.3 (14.2)	2276.9 (7.4)	652.9 (25.9)
(50 K).....	2340.4 (12.8)	2276.5 (6.8)	653.9 (21.0)
(100 K).....	2339.6 (10.2)	2275.5 (5.7)	654.0 (19.4)
(140 K).....	2339.4 (9.2)	2275.1 (5.0)	653.7 (18.2)
(150 K).....	2339.3 (9.1)	2275.1 (4.3)	654.2 (17.6)
$H_2O:CO_2 = 5:1$			
(10 K).....	2339.8 (24.6)	2278.9 (7.0)	654.0 (23.1)
(50 K).....	2338.9 (23.1)	2278.2 (7.7)	654.1 (21.2)
(85 K).....	2338.8 (19.4)	2277.5 (8.3)	654.6 (18.1)
(100 K).....	2338.6 (16.8)	2277.2 (8.9)	654.8 (17.2)
(150 K).....	2337.4 (11.9)	2282.0, 2274.8 (3.7, 6.5)	655.4 (14.4)
$H_2O:CO_2 = 1:1$			
(10 K).....	2328.7 (29.9)	2279.8 (8.6)	654.7 (10.0)
(50 K).....	2343.1 (11.0)	2282.3 (2.2)	659.6, 654.5 (3.3, 2.8)
(85 K).....	2343.2 (10.2)	2282.3 (2.4)	659.7, 654.7 (2.6, 2.2)
(100 K).....	2340.1 (8.0)	...[d]	...[d]
(150 K).....	...[d]	...[d]	...[d]
$H_2O:CH_3OH:CO_2 = 20:10:1$			
(10 K).....	2341.4 (9.5)	2276.4 (6.3)	658.3, 650.5 (28.8)[e]
(20 K).....	2341.4 (9.4)	2276.1 (6.1)	659.2, 650.0 (25.4)[e]
(50 K).....	2340.7 (8.7)	2275.6 (5.0)	657.6, 650.2 (24.1)[e]
(100 K).....	2340.0 (7.3)	2274.7 (4.5)	656.9, 650.3 (21.7)[e]
(140 K).....	2345.8 (5.5)[e]	2280.0 (5.1)[e]	655.8 (10.5)
(150 K).....	2345.9 (5.2)[e]	2280.0 (4.5)[e]	656.0 (10.6)

[a] Measured on percent transmission spectra.

[b] At 10 K, this band has an intense shoulder at about 2325 cm^{-1} which decreases rapidly in strength with temperature (see Fig. 3).

[c] Doublet which is not fully separated. FWHM represents the widths of the entire doublet.

[d] H_2O dominates the spectrum; all CO_2 lost by 125 K.

[e] Band contains a moderate shoulder at the same position of the main band seen at 100 K. See text and Fig. 3.

uous flow. Pulsed deposition produces a slightly annealed sample (Allamandola, Lucas, and Pimentel 1978). Thus, the molecular orientations responsible for the low-frequency shoulder in the 10 K spectrum of pure CO_2 in Figure 3 are probably very unstable.

The $H_2O:CH_3OH:CO_2 = 20:10:1$ interstellar ice analog also deserves special comment. At temperatures below 100 K, the feature produced by this ice mixture behaves much like that of the $H_2O:CO_2 = 20:1$ mixture, although it is slightly narrower. Between 100 and 140 K, however, the feature undergoes a radical change. The band near 2340 cm^{-1} decreases substantially in strength while a new band grows near 2346 cm^{-1} (see Fig. 3). This new band position is near the CO_2 gas phase position, suggesting that the presence of the CH_3OH has allowed the ice to anneal into a crystalline form containing a substantial number of larger sites involving CH_3OH in which the CO_2 is trapped. This interpretation is supported by other spectral evidence as well. Between 100 and 150 K, the intense CH_3OH band near 1010 cm^{-1} (9.90 μm) begins to split, a weak band near 1435 cm^{-1} (6.97 μm) increases in intensity, the OH stretch band at 3250 cm^{-1} (3.08 μm) starts to transform into its crystalline profile, and the peak of the H_2O librational mode,

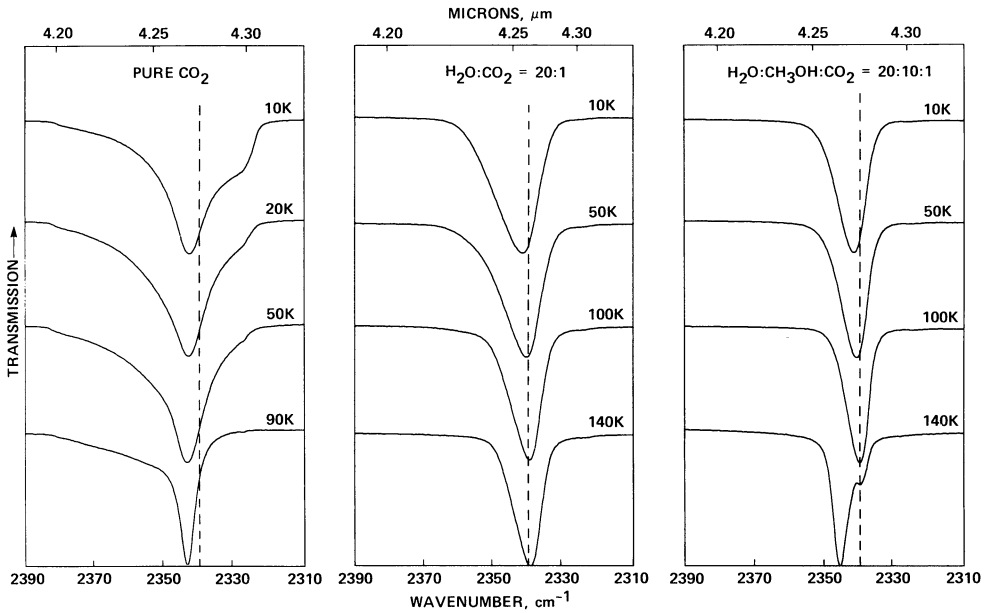

FIG. 3.—The dependence of the $^{12}CO_2$ ν_3 band on temperature for three different matrix compositions. All the ices were deposited at 10 K. Spectra were taken at the temperatures listed after warming at a rate of 2 K per minute. A dashed line is provided at 2340 cm^{-1} for reference.

which falls near 750 cm^{-1} (13.3 μm) at 20 K, peaks closer to 820 cm^{-1} (12.2 μm).

2. *The $^{13}CO_2$ asymmetric stretching fundamental* (ν_3).—In good signal-to-noise spectra, it was possible to measure the ν_3 $^{13}CO_2$ asymmetric stretching fundamental band near 2280 cm^{-1} (4.39 μm) (Fig. 4). This band is due to the same vibrational mode as the 2340 cm^{-1} band but is shifted to lower frequency by the larger mass of the ^{13}C atom. A summary of band position and width as a function of temperature and matrix composition is given in Table 1. The FWHM of the $^{13}CO_2$ band is always narrower than the corresponding $^{12}CO_2$ band, presumably because the vibration is decoupled from the other CO_2 molecules in the matrix (Falk 1987). Not surprisingly, this effect is most noticeable in the pure CO_2 ices.

In all other respects, the $^{13}CO_2$ asymmetric stretch band behaves like its $^{12}CO_2$ counterpart. The presence of surrounding molecules lowers the frequency of the $^{13}CO_2$ band with respect to its gas phase position by a similar amount to that observed for the $^{12}CO_2$ band in the same matrix. $^{13}CO_2$ band width and position variations with increased temperature also mimic those of the $^{12}CO_2$ band. As with the $^{12}CO_2$ fundamental, our reported peak positions differ by a few wavenumbers from those reported in Falk (1987). As before, we attribute this to the difference in deposition techniques.

In order to test whether the $^{13}CO_2$ and $^{12}CO_2$ bands can be used to quantify their ratios in interstellar ices, the strength of the $^{13}CO_2$ stretch band relative to the $^{12}CO_2$ stretch band was determined for all the ices listed in Table 1. The relative strength of these two bands varied slightly for CO_2 in different matrices but was constant and temperature independent within any given matrix. Table 2 lists the observed band strength ratios for the various ice mixtures given in Table 1. Assuming that the CO_2 in our experiments had a terrestrial $^{13}C/^{12}C$ ratio of 0.0112, it is possible to derive the correction coefficients for each ice matrix (also listed in Table 2). Langenscheidt, Patnaik, and Roessler (1990) have measured the dependence of this ratio on CO_2 concentration in several ices.

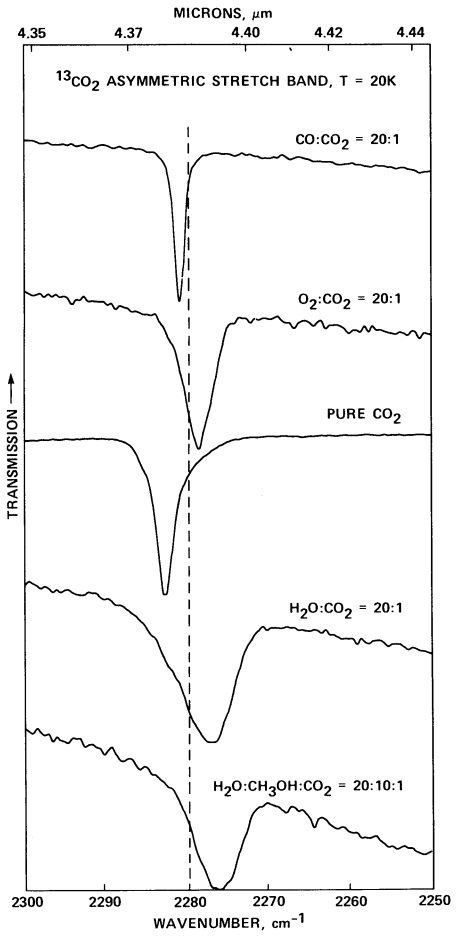

FIG. 4.—The $^{13}CO_2$ ν_3 band produced by the asymmetric stretching vibrations of $^{13}CO_2$ in different matrices. All the ices were deposited at 10 K and warmed to 20 K. A dashed line is provided at 2280 cm^{-1} for reference.

TABLE 2

RELATIVE STRENGTHS OF THE $^{13}CO_2$ AND $^{12}CO_2$ BANDS IN SEVERAL ICE MATRICES

Ice Mixture	Integrated Band Ratio[a] ($^{13}CO_2/^{12}CO_2$)	Number of Measurements	Correction Factor[b]
$CO:CO_2 = 20:1$	0.0105 ± 0.0005	2	1.07
$O_2:CO_2 = 20:1$	0.0099 ± 0.0004	2	1.13
Pure CO_2	0.0118 ± 0.0003	5	0.95
$H_2O:CO_2 > 20:1$	0.0096 ± 0.0008	12	1.17
$H_2O:CO_2 = 5:1$	0.0104 ± 0.0002[c]	4	1.08[c]
$H_2O:CO_2 = 1:1$	0.0129 ± 0.0007[d]	3	0.87[d]
$H_2O:CH_3OH:CO_2 = 20:10:1$	0.0091 ± 0.0006	6	1.23

[a] Listed errors represent the standard deviation of the derived values.

[b] Assumes the CO_2 used had a terrestrial $^{13}C/^{12}C$ ratio of 0.0112.

[c] Value valid below 100 K. Above 100 K, substantial CO_2 loss occurs and the value alters to that of $H_2O/CO_2 > 20$ ices. (See Langenscheidt, Patnaik, and Roessler 1990 for a discussion of concentration dependence).

[d] Value valid below 85 K. Above 85 K, substantial CO_2 loss occurs and the value alters to that of $H_2O/CO_2 > 20$ ices.

These data show that it should be possible to use astronomical observations of the $^{13}CO_2$ and $^{12}CO_2$ bands to determine the $^{13}C/^{12}C$ distribution in this molecule to about 20%. If the matrix composition is known from band position and width information, it should be possible to determine this ratio more accurately.

3. *The CO_2 bending fundamental (ν_2).*—The CO_2 bending fundamental falls near 660 cm^{-1} (15.2 μm). This vibration is doubly degenerate, and the band splits when the axial symmetry of the molecule is broken (see Tso and Lee 1985*a*). As a result, this band should be especially sensitive to matrix composition. The band positions, widths, and profiles in several matrices are given in Table 1 and Figure 5. Note the weak $^{18}O^{12}C^{16}O$ band near 640 cm^{-1} in pure CO_2.

The bending fundamental also falls at lower frequencies than the central value for gas phase CO_2 (667.7 cm^{-1}), in this case by 6–18 cm^{-1}. The magnitude of this shift is not related in any simple way to the magnitude of the shift of the stretching mode. In most cases, the degeneracy of the vibration is broken by the matrix. This is particularly obvious for the pure CO_2 ices, but a double-peaked structure is evident in the $CO:CO_2$ and $O_2:CO_2$ ices as well. The band splitting in the $CO:CO_2$ ice is more obvious at 10 K. Our results for the pure CO_2 ice are similar to those of Guasti, Schettino, and Brigot (1978) but differ somewhat from those of Falk (1987). In Falk's pulse-deposited CO_2 ice band splitting does not occur at 10 K, although it does at higher temperatures.

As with the stretching mode bands, warm-up of the ices generally sharpens the bands and can result in minor but systematic shifts in the band positions (Table 1 and Fig. 6). Again, O_2 matrices are an exception, producing increased widths as the temperature is warmed from 10 to 20 K.

The behavior of the bending mode band in the $H_2O:CH_3OH:CO_2$ interstellar ice analog between 100 and 140 K is analogous to that of the stretching mode band. The 10 K spectrum indicates that CO_2 is trapped in two different sites producing bands at 659 cm^{-1} (15.17 μm) and 650 cm^{-1} (15.38 μm). These two sites appear to contain roughly equal amounts of CO_2 up to 100 K but by 140 K, the majority of the CO_2 has shifted into the 659 cm^{-1} site. This shift to higher frequencies (closer to the gas phase value) is consistent with the inference from the behavior of the stretching band that this ice is annealing into a form containing relatively larger sites for the CO_2 to reside in.

Finally, it is important to keep in mind that the degeneracy of this band does not split in the polar, H_2O-rich ices, whereas it does in the nonpolar ices. Analysis of the solid CO band has

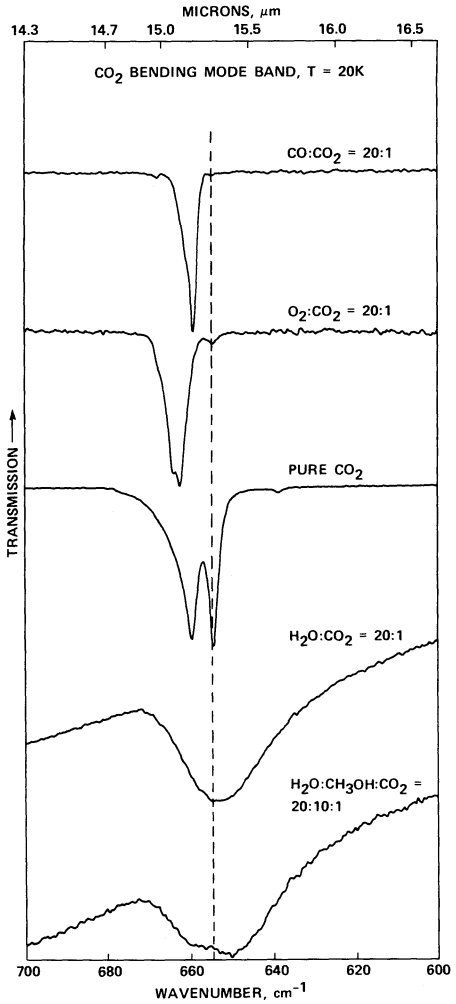

FIG. 5.—The CO_2 ν_2 band produced by the bending mode of CO_2 in different matrices. All the ices were deposited at 10 K and warmed to 20 K. A dashed line is provided at 655 cm^{-1} for reference. Note the weak band due to $^{18}O^{12}C^{16}O$ at about 640 cm^{-1} in the spectrum of the pure CO_2 ice.

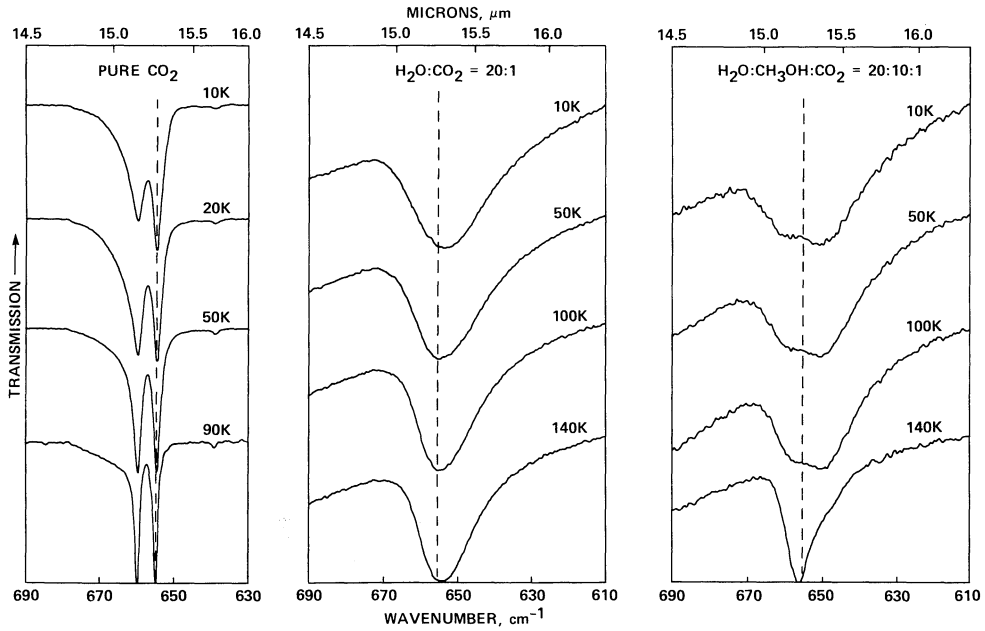

FIG. 6.—The dependence of the CO_2 ν_2 band on temperature in three different ices. All the ices were deposited at 10 K. Spectra were taken at the temperatures listed after the ices had been warmed to these temperatures at a rate of 2 K per minute. A dashed line is provided at 655 cm^{-1} for reference.

shown that these two different classes of ice are present in different regions of interstellar clouds (Sandford *et al.* 1988). Thus, the CO_2 bending mode band may prove to be a very useful probe of these different regimes in interstellar clouds.

4. *The* $(\nu_1 + \nu_3)$ CO_2 *combination band.*—This weak band is produced by a combination of the symmetric (ν_1) and asymmetric (ν_3) CO_2 stretching vibrations and occurs near 3705 cm^{-1} (2.70 μm). The ν_1 symmetric stretching vibration, which occurs at about 1385 cm^{-1} (7.22 μm), is infrared inactive (see Falk and Seto 1986). A summary of the band position and width as a function of matrix composition and temperature is given in Table 3. This band displays similarities to the previously discussed CO_2 bands in that (1) its position is matrix dependent and H_2O-rich ices produce the largest shifts to lower frequencies, (2) the FWHM is matrix dependent and is widest for H_2O-rich ices, and (3) the band generally grows narrower as the ice is warmed (although CO_2 in O_2 is still an exception).

This band is difficult to study in H_2O-rich ices because it is weak, it falls on the shoulder of the strong "3.0" μm O—H stretch band, and it sometimes overlaps with the "free-OH" band that falls near 2630 cm^{-1} (2.76 μm).

5. *The* $(2\nu_2 + \nu_3)$ CO_2 *combination/overtone band.*—This band, which falls near 3600 cm^{-1} (2.78 μm), is produced by a combination of the first overtone of the CO_2 bending vibration (ν_2) with the asymmetric CO_2 stretching vibration (ν_3). Since it involves three excitations, it is weaker than the $\nu_1 + \nu_3$ combination band.

This band is unobservable in ices dominated by H_2O since it falls on the steepest part of the slope on the side of the "3.0" μm H_2O ice band and is usually blended with the "free-OH" vibration (Tso and Lee 1985*b*). As far as can be determined, this band follows the general trends observed for the other CO_2 bands, i.e., the band's position and widths are matrix and temperature dependent and widths generally decrease during warm-up, except in O_2 matrices.

6. *The spectral effects of deposition temperature.*—Since H_2O-rich ices containing CO_2 are expected to be formed and processed in a wide variety of environments in the interstellar medium and in comets, a series of depositions were carried out at temperatures of 10, 30, 70, 80, 90, and 100 K for the H_2O:CO_2 = 20:1 ices in order to investigate the effect of deposition temperature on the CO_2 fundamentals. Samples were not deposited above 100 K, since CO_2 did not stick in H_2O matrices above this temperature under our laboratory conditions. Figure 7 shows the profile of the CO_2 asymmetric stretching band as a function of deposition temperature.

Comparison of Figures 3 and 7 illustrates that deposition at higher temperatures results in narrower bands at any given temperature. This can be understood in terms of the kinetics of the annealing process. For a molecule to change its orientation inside a solid during annealing, it must overcome an energy activation barrier. During deposition, however, some annealing can occur at the surface, where the activation barrier for rearrangement is lower than in the bulk. Consequently, a matrix that is deposited at low temperature and subsequently annealed at a higher temperature will be less ordered (and produce broader bands) than one directly deposited at the higher temperature.

A new feature, not seen in the 10 K depositions with their subsequent warm-ups, is apparent as a shoulder centered near 2365 cm^{-1} (4.228 μm) in ices deposited between 50 and 80 K. This feature is presumably due to CO_2 trapped in a site unique to partially ordered amorphous H_2O ices.

7. *The spectral effects of* CO_2 *concentration.*—To probe the effect of concentration on the five CO_2 bands, H_2O:CO_2 ices having ratios of 50, 20, 5, and 1 were made at 10 K. Each ice was then warmed at 2 K per minute, and spectra were taken at higher temperatures. A summary of the positions and widths for the five bands produced by these ices can be found in Tables 1 and 3. Figure 8 shows the $^{12}CO_2$ asymmetric stretching bands from these experiments.

TABLE 3

POSITION AND WIDTH OF THE ($\nu_1 + \nu_3$) AND ($2\nu_2 + \nu_3$) CO_2 COMBINATION BANDS IN VARIOUS ICE MIXTURES

Ice Composition	($\nu_1 + \nu_3$) Peak and FWHM[a] (cm^{-1})	($2\nu_2 + \nu_3$) Peak and FWHM[a] (cm^{-1})
CO_2		
(10 K).....	3707.8 (3.1)	3599.5 (2.0)
(20 K).....	3707.9 (3.0)	3599.5 (2.0)
(50 K).....	3707.9 (2.4)	3599.5 (1.7)
(80 K).....	3707.5 (1.6)	3599.5 (1.3)
$CO:CO_2 = 20:1$		
(10 K).....	3707.5 (2.4)	3602.1 (2.4)
(20 K).....	3707.0 (2.1)	3601.4 (2.2)
$O_2:CO_2 = 20:1$		
(10 K).....	3704.5 (4.8)	3600.6 (3.9)
(20 K).....	3705.8 (5.4)	3601.7 (5.4)
$H_2O:CO_2 = 50:1$		
(10 K).....	3697 (16)	...
(50 K).....	3696 (12)	...
(100 K).....	3697 (11)	...
(150 K).....	3697 (13)	...
$H_2O:CO_2 = 20:1$		
(10 K).....	3698 (14)	...
(20 K).....	3698 (15)	...
(50 K).....	3698 (14)	...
(100 K).....	3696 (13)	...
(140 K).....	3696 (10)	...
(150 K).....	3696 (11)	...
$H_2O:CO_2 = 5:1$		
(10 K).....	3702.9 (12.7)	...
(50 K).....	3701.9 (11.6)	...
(85 K).....	3702.1 (14.8)	...
(100 K).....	3701.3 (15.6)	...
(150 K).....	3707.7, 3695.6 (2.2, 9.1)	...
$H_2O:CO_2 = 1:1$		
(10 K).....	3703.0 (10.6)	3595.9 (7.2)
(50 K).....	3707.4, 3683.3 (2.5, 13.7)	3599.4 (1.8)
(85 K).....	3707.6 (1.9)	3599.5 (1.5)
(100 K).....	...[b]	...[b]
(150 K).....	...[b]	...[b]
$H_2O:CH_3OH:CO_2 = 20:10:1$		
(10 K).....	3700.2 (14.1)	...
(20 K).....	3698.7 (14.8)	...
(50 K).....	3697.3 (11.2)	...
(100 K).....	3695.9 (9.5)	...
(140 K).....	3702.9 (7.7)	...
(150 K).....	3703.7 (9.6)	...

[a] Measured on percent transmission spectra.
[b] H_2O dominates the spectrum; all CO_2 lost by 125 K.

The results are complex although several patterns are apparent. First, most bands still grow narrower as the ice is annealed, the only exceptions being the $^{13}CO_2$ ν_3 stretch and ($\nu_1 + \nu_3$) combination bands in the 5:1 ice (not shown). However, the band splitting in the 150 K warm-up spectrum of this ice indicates that the CO_2 falls into one of two distinct matrix sites as the ice anneals. Thus, the apparent increasing FWHM of the $^{13}CO_2$ and ($\nu_1 + \nu_3$) bands may actually be due to the progressive blending of two adjacent features. Second, all the ν_3 asymmetric stretch bands shift to lower frequencies as the ices are warmed, except for the 10–50 K warm-up of the 1:1 ice. In the 1:1 ice at 10 K, the band peaks at the position of the strong low-frequency shoulder in the spectrum of pure CO_2 ice at 10 K (Fig. 3). Again, we attribute this to CO_2 in a very unstable site in the amorphous ice, since it is quickly removed by warming to 50 K. Finally, at temperatures above 50 K,

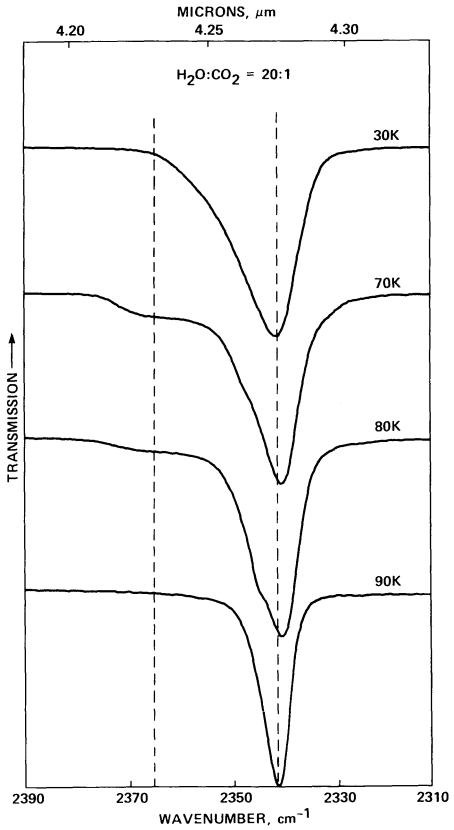

FIG. 7.—The $^{12}CO_2$ ν_3 fundamental band in $H_2O:CO_2$ ices as a function of deposition temperature. Each ice was prepared by deposition of an $H_2O:CO_2 = 20:1$ gas on the window at the listed temperatures. The 50 K deposition band profile (not shown) is similar to the 70 K profile. The 10 K profile is similar to that at 30 K (Fig. 3). Dashed lines are provided at 2340 and 2356 cm^{-1} for reference.

bandwidths seem to be smaller at the CO_2-rich and CO_2-poor extremes.

ii) CO_2 *Absorption Band Strengths*

The column density N (cm^{-2}) of an infrared band carrier can be determined using the equation

$$N = \frac{\int \tau_\nu \, d\nu}{A} \simeq \frac{\tau_{\max} \Delta\nu_{1/2}}{A}, \quad (1)$$

where $\tau_{\max}$ is the optical depth of the band at maximum absorbance, $\Delta\nu_{1/2}$ is the FWHM of the band (measured in absorbance) in cm^{-1}, and A is the integrated absorbance of the band in cm per molecule. There can be large infrared intensity differences between vibrational transitions of a molecule in the gas phase and those same vibrations when the molecule is in the solid phase. Similar differences can also occur when the molecule is in matrices with different compositions. Consequently, the column density of an individual component in an interstellar ice can only be accurately determined using the A values measured in realistic ice analogs. In view of the probable occurrence of CO_2 frozen in H_2O-rich as well as nonpolar ices in the interstellar medium and comets, we have experimentally determined the A values of the five infrared CO_2 bands for CO_2 in H_2O and CO matrices and in pure CO_2 ices.

The A values for the asymmetric stretching fundamental (ν_3) of $^{12}CO_2$ in pure CO_2 ice has previously been determined to be

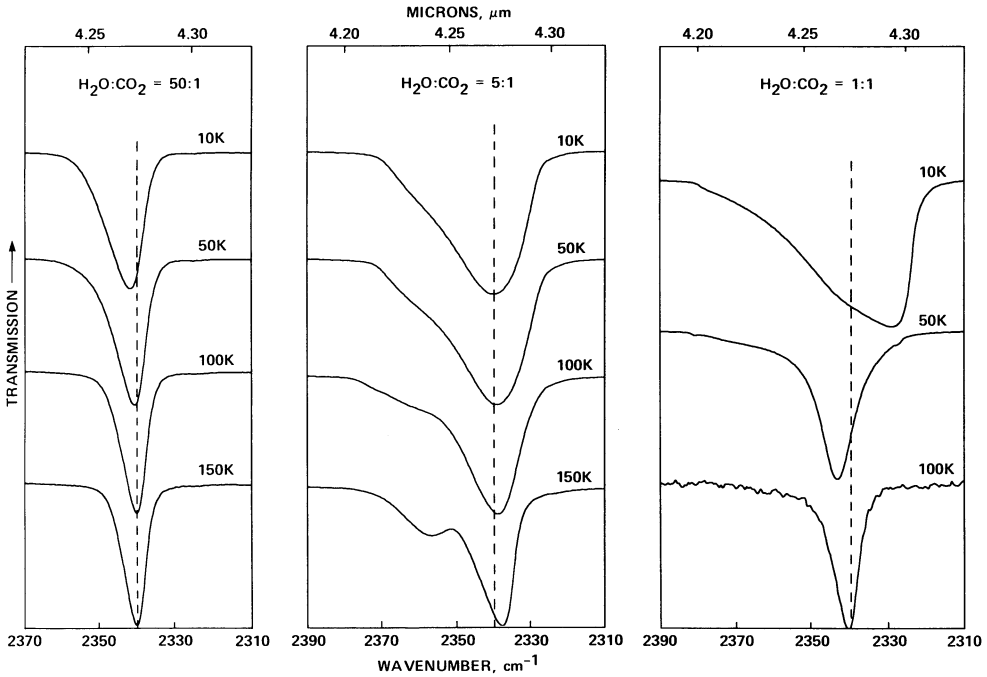

FIG. 8.—The $^{12}CO_2$ ν_3 fundamental band in H_2O:CO_2 ices as a function of CO_2 concentration. Similar spectra for a 20:1 ice can be found in Fig. 3. The ices were prepared at 10 K and subsequently warmed at 2 K per minute to the temperatures listed. A dashed line is provided at 2340 cm^{-1} for reference.

7.6×10^{-17} cm per molecule (Yamada and Person 1964). Using this value, we derive the A values for the other bands in pure CO_2 by simple scaling of the relative integrated band areas. The results are given in Table 4. A series of experiments in which pure CO_2 ices were repeatedly warmed and recooled between 10 and 80 K demonstrated that the A values for all five bands are temperature independent to the 10% level with the exception of the bending mode, which appears to increase by about 2% per 10 K temperature increase.

We previously determined that $A_{CO_2} = 2.1 \times 10^{-16}$ cm per molecule for the $^{12}CO_2$ stretching mode and $A_{CO_2} = 4.1 \times 10^{-17}$ for the bending mode in H_2O:CO_2 = 20:1 ices (Sandford *et al.* 1988). The A values for the other bands can be determined by scaling integrated band areas and are given in Table 4. We note that the A values from Sandford *et al.* (1988) for CO_2 in H_2O-rich ices are about a factor of 4 larger than those estimated previously by d'Hendecourt and Allamandola (1986). This difference is presumably due to saturation effects in the earlier work. Therefore, the A values for CO_2 reported here and in Sandford *et al.* (1988) are the better values.

A series of experiments in which H_2CO:CO_2 = 20:1 ices were repeatedly warmed and recooled between 10 and 150 K demonstrated that the A values for the five CO_2 bands show minor temperature dependence when the CO_2 is in an H_2O matrix. The A value for the $^{12}CO_2$ and $^{13}CO_2$ stretching mode bands and the $(\nu_1 + \nu_3)$ and $(2\nu_2 + \nu_3)$ combination bands all decrease slightly with temperature while the A value for the CO_2 bending mode increases slightly. The inferred temperature dependences are listed in Table 4.

CO_2 A values were also derived from the CO:CO_2 = 20:1 ice spectra. In ices this rich in CO we have assumed that the A_{CO} value will be that of pure CO, i.e., $A_{CO} = 1.0 \times 10^{-17}$ cm per molecule for the CO stretch band. The A values for the five CO_2 bands were then determined by scaling integrated band areas to the area of the 2139 cm^{-1} CO band and assuming $CO/CO_2 = 20$. The results of these calculations are also given in Table 4.

b) *The Vaporization-Condensation Behavior of CO_2-bearing Ices*

In this section, the results of a number of experiments designed to investigate the vaporization and condensation behavior of CO_2 in astrophysical ice analogs are presented. First we determine the surface binding energy of a CO_2 molecule on the surface of pure solid CO_2. This is followed by a measurement of the efficiency with which CO_2 sticks to H_2O ices as a function of temperature. These results are then used to derive an effective CO_2-H_2O surface binding energy. Finally, we end the section with a discussion of the CO_2 loss behavior from H_2O-rich ices during thermal warm-up. The astrophysical consequences of these results are discussed in § IV.

i) *The Surface and Volume Binding Energies of CO_2 in Pure CO_2 Ice*

Pure CO_2, when deposited at 10 K and warmed steadily at the rate of 2 K per minute, begins to sublime at appreciable rates at temperatures above 80 K. In a pair of experiments, CO_2 ices were deposited at 10 K and warmed at 2 K per minute to temperatures of 80 and 83 K, respectively. The ices were then maintained at these temperatures while the CO_2 sublimation was periodically monitored by measuring the area of the 2342.7 cm^{-1} asymmetric stretch band. The 80 K ice was monitored for 107 minutes, and a loss rate of 3.5×10^{12} molecules s^{-1} was determined. The 83 K ice was monitored for 38 minutes, and a loss rate of 2.1×10^{13} molecules s^{-1} was measured.

The observed deposition-sublimation behavior is consistent with the models of Langmuir (1916) and Frenkel (1924), in which it is assumed that the sticking efficiency is equal to 1.0

TABLE 4

CO_2 INTEGRATED BAND INTENSITIES

Ice[a]	Mode	Band Position (cm^{-1}) (μm)	A (cm per molecule)
CO_2	(ν_3) $^{12}C{=}O$ stretch	2343 (4.268)	7.6×10^{-17}[b]
	(ν_3) $^{13}C{=}O$ stretch	2283 (4.380)	9.0×10^{-19}
	(ν_2) $O{=}C{=}O$ bend	660, 665 (15.15, 15.27)	1.1×10^{-17}[c]
	($\nu_1 + \nu_3$) combination	3708 (2.697)	1.2×10^{-18}
	($2\nu_2 + \nu_3$) combination	3600 (2.778)	4.1×10^{-19}
$H_2O{:}CO_2$ (20:1)	(ν_3) $^{12}C{=}O$ stretch	2342 (4.270)	2.1×10^{-16}[d]
	(ν_3) $^{13}C{=}O$ stretch	2277 (4.392)	2.0×10^{-18}[e]
	(ν_2) $O{=}C{=}O$ bend	653 (15.31)	4.1×10^{-17}[f]
	($\nu_1 + \nu_3$) combination	3698 (2.704)	2.3×10^{-18}[g]
	($2\nu_2 + \nu_3$) combination	...	...[h]
$CO{:}CO_2$ (20:1)	(ν_3) $^{12}C{=}O$ stretch	2346 (4.263)	7.4×10^{-17}
	(ν_3) $^{13}C{=}O$ stretch	2281 (4.384)	7.8×10^{-19}
	(ν_2) $O{=}C{=}O$ bend	659 (15.18)	7.6×10^{-18}
	($\nu_1 + \nu_3$) combination	3708 (2.697)	1.5×10^{-18}
	($2\nu_2 + \nu_3$) combination	3602 (2.776)	6.6×10^{-19}

[a] Values for the CO_2, H_2O, and CO matrices represent the average of measurements from five, six, and four different experiments, respectively.

[b] Value from Yamada and Person 1964.

[c] Value for both bands combined and is appropriate for 10 K. The A value increases by about 2% per 10 K as the temperature increases.

[d] Value from Sandford *et al.* 1988 and appropriate for 10 K. The A value decreases with temperature increase by about 0.5% per 10 K.

[e] Value appropriate for 10 K. The A value decreases with temperature increase by about 0.5% per 10 K.

[f] Value for Sandford *et al.* 1988 and appropriate for 10 K. The A value increases with temperature increase by about 0.5% per 10 K.

[g] Value only accurate to about 20% because of uncertainties associated with the changing background due to the adjacent H_2O band. The A value decreases with temperature increase by roughly 2% per 10 K.

[h] Band cannot be seen due to overlap with the strong H_2O band.

and that reevaporation takes place at a rate given by the equation

$$R_s = \nu_0 \exp(-\Delta H_s/kT), \quad (2)$$

where ν_0 is the lattice vibrational frequency of the CO_2 molecule within the CO_2 matrix, ΔH_s is the binding energy of the CO_2 to a surface site on the matrix, k is the Boltzmann constant, and T is the ice temperature in K. As discussed in detail in Sandford and Allamandola (1988), it is then possible to calculate the CO_2-CO_2 surface binding energy using the equation

$$\frac{\Delta H_s}{k} = -T \ln\left\{\frac{a_m}{\nu_0 t_f A_{CO_2}}[(\tau\Delta\nu)_i - (\tau\Delta\nu)_f]\right\}, \quad (3)$$

where a_m is the area of a CO_2 molecular site, t_f is the time over which the loss rate is measured, $(\tau\Delta\nu)_i$ is the integrated band strength at time $t_i = 0$, $(\tau\Delta\nu)_f$ is the integrated band strength at time t_f, and A_{CO_2} is the integrated absorbance of the solid CO_2 band in cm per molecule.

The size of the CO_2 lattice site in CO_2 ice is $5.32 \times 3.00 \times 3.00$ Å (Barrett and Meyer 1965), implying a mean site area of $a_m = 15.5$ Å^2. Solid CO_2 has lattice vibrations that produce infrared absorption bands at 68 and 114 cm^{-1} (Anderson and Walmsley 1964; Ron and Schnepp 1967) and Raman bands at 73.5, 91.5, and 132 Δcm^{-1} (Cahill and Leroi 1969). These correspond to an average ν_0 value of 2.9×10^{12} s^{-1}. A_{CO_2} for the CO_2 asymmetric stretching fundamental in solid CO_2 is 7.6×10^{-17} cm per molecule (Yamada and Person 1964).

These parameter values and the observed CO_2 loss rates were used in equation (3) to calculate the surface binding energy of CO_2 on solid CO_2. The formalism of expressing binding strengths in terms of $(\Delta H_s/k)$, i.e., in K, will be used in this paper. The mean CO_2-CO_2 surface binding energy derived from five measurements at 80 K and six measurements at 83 K is $(\Delta H_s/k) = 2690 \pm 50$ K. This value falls in the range of previously reported values for the heat of sublimation of 2350 K (Leighton and Murray 1966) and 3010 K (Smith 1929).

ii) *The CO_2 Sticking Efficiency in H_2O Ice*

The temperature dependence of the sticking efficiency of CO_2 on H_2O ice was determined by depositing an $H_2O{:}CO_2 = 20{:}1$ gas mixture on a CsI window held at a series of different temperatures. After deposition, the H_2O/CO_2 ratio was determined using the 3290 cm^{-1} ("3.0" μm) H_2O band and the 2342 cm^{-1} (4.270 μm) CO_2 band. Figure 9 shows a plot of the derived CO_2 sticking efficiency as a function of substrate temperature. In preparing this plot, it was assumed that both H_2O and CO_2 stick with 100% efficiency at 10 K.

Under our experimental conditions, measurable amounts of CO_2 can still be condensed out of the gas phase at temperatures up to 100 K in the presence of H_2O. This is only slightly higher than the temperature at which pure CO_2 condenses in similar experiments (about 85 K). Of course, the exact upper temperature limit to the CO_2 sticking will depend on variables such as the deposition rate, temperature of the incoming gas, thermal conductivity of the ice sample, and the pressure in the cell.

iii) *The CO_2 Surface Binding Energy on H_2O Ices*

The fact that the CO_2 sticking efficiency on H_2O drops to zero at about the same temperature at which pure CO_2 sub-

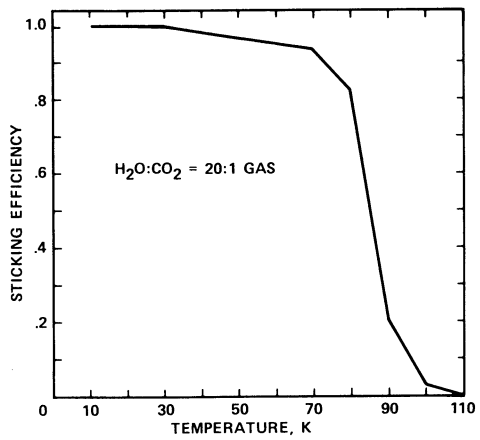

FIG. 9.—The sticking efficiency of CO_2 on H_2O ices as a function of temperature. The sticking efficiencies were calculated assuming CO_2 sticks with 100% efficiency at 10 K.

limes implies that the surface binding energies of CO_2 on H_2O are similar. In order to quantify this, an attempt was made to derive the CO_2-H_2O volume binding energy with a diffusion technique previously used on H_2O:CO ices (Sandford and Allamandola 1988). Unfortunately, CO_2 loss rates from $H_2O:CO_2 = 20:1$ ices were to low, even at 150 K, for the diffusion technique to be used (see the next section). Instead, we derive a rough surface binding energy from sticking efficiency data presented in the previous section.

At the deposition rate used in the sticking efficiency experiments (about 1×10^{15} molecules s^{-1} in the infrared beam), each surface site received about 15 new molecules per second. Each CO_2 molecule therefore undergoes about 2×10^{11} vibrations within its surface site before the next monolayer of molecules is deposited and thus has ample opportunity to leave the surface before the next monolayer is deposited. Therefore, CO_2 trapping is not due to large numbers of H_2O molecules piling onto the CO_2 molecules before they can "rebound" from the ice, and the sticking efficiencies of the previous section can be used to derive the surface binding energy of CO_2 on H_2O ices.

The time a molecule resides on the surface of an ice during deposition is given by the reciprocal of equation (2). Solving this reciprocal for the surface binding energy yields

$$\frac{\Delta H_s}{k} = T \ln(\nu_0 t) . \quad (4)$$

If we let T equal the lowest temperature at which the sticking efficiency of CO_2 is zero (i.e., the temperature at which the CO_2 molecules leave the surface at the same rate they are arriving during deposition), then t is the time between the deposition of successive monolayers. Using equation (4) with the parameters appropriate to our $H_2O:CO_2$ depositions ($t = 0.067$ s, $\nu_0 = 2.9 \times 10^{12}$ s^{-1}, and $T = 110$ K [see Fig. 9]) yields a CO_2-H_2O surface binding energy of $\Delta H_s/k = 2860$ K. This value is slightly higher than the CO_2-CO_2 surface binding energy value derived earlier and is qualitatively consistent with the observation that CO_2 freezes out at slightly higher temperatures in our experiments when H_2O is present. Taking into account the uncertainties associated with the deposition rate, ν_0, and the exact temperature at which the sticking efficiency goes to zero, the stated value of $\Delta H_s/k = 2860$ K is expected to be accurate to, conservatively, about 200 K.

This technique was used to calculate the surface binding energy of CO on H_2O using sticking efficiencies reported earlier in Sandford and Allamandola (1988). Using the values of $t = 0.2$ s, $\nu = 2.0 \times 10^{12}$ s^{-1}, and $T = 65$ K appropriate for the earlier H_2O:CO experiments, we derive a CO-H_2O surface binding energy of $\Delta H_s/k = 1740$ K. This value is considerably lower than our previous value of 3500 K estimated from our reliable volume binding energy by making the standard (but now obviously questionable) assumption that the binding energy of a molecule scales as the number of its nearest neighbors.

The residence times of CO, CO_2, and H_2O on various ices are listed in Table 5 for a range of temperatures. The lower temperatures are of interest for ices in interstellar clouds, while the higher temperatures are of interest to cometary applications. The residence times for CO listed in Table 5 were calculated using the more appropriate surface binding energy of 1740 K, and Table 5 therefore supercedes Table 4 of Sandford and Allamandola (1988).

iv) CO_2 *Loss from* H_2O *Matrices During Warming*

CO_2 loss from H_2O matrices was investigated by monitoring the decrease in the CO_2 asymmetric stretch band in the spectra of $H_2O:CO_2$ ices as they were warmed. The minor temperature dependence of the absorption strength of this band (§ III*a*[ii]) was taken into account. These studies were carried out on ices with H_2O/CO_2 ratios of 50, 20, 5, and 1. Each gas mixture was deposited at 10 K and then warmed to successively higher temperatures at a rate of 2 K per minute. The warm-up was temporarily halted while each spectrum was taken. Once the ice reached 150 K, its spectrum was monitored as a function of time to examine CO_2 loss during the H_2O amorphous-to-cubic ice transformation and subsequent sublimation. Samples were not warmed above 150 K, the point at which H_2O sublimation became very rapid.

CO_2 loss from H_2O-rich matrices is complex and differs substantially from that for CO in H_2O (Sandford and Allamandola 1988). The loss of CO_2 from H_2O matrices is highly concentration dependent, exhibiting one behavior for H_2O/CO_2 ratios above 20 and another for lower ratios.

There was no appreciable CO_2 loss (<10%) from the $H_2O:CO_2 = 50:1$ and 20:1 ices below 140 K. Warm-up of these ices to 150 K resulted in little immediate CO loss, but approximately 20% of the original CO_2 left during the following 20 minutes as the ice was maintained at 150 K. After 20 minutes, the CO_2 loss rate dropped to that of the subliming H_2O. During the time the CO_2 was observed to leave at an accelerated rate, the 3290 cm^{-1} (3.0 μm) H_2O band profile changed from that of a relatively amorphous ice to that of cubic ice. These data suggest that at concentrations of 5% and lower, CO_2 is physically trapped in the strong, hydrogen-bonded, amorphous H_2O lattice. Little CO_2 is lost except during the H_2O amorphous-to-cubic ice phase transition, which only proceeds at a significant rate above 140 K. The excess energy liberated by the phase transitions and the minor movement of the H_2O as it realigns itself allows some CO_2 to escape. Once the H_2O ice has fully annealed, the CO_2 is again physically trapped in the ice and is not released until the entrapping H_2O sublimes away. Thus, the loss of CO_2 from ices having $H_2O/CO_2 > 20$ is entirely controlled by the H_2O. This behavior is in sharp contrast to that of CO trapped in H_2O. CO can diffuse through the H_2O lattice, and a substantial fraction of it can escape at temperatures well below 150 K.

TABLE 5A

COMPARISON OF CO, CO_2, AND H_2O RESIDENCE TIMES ON VARIOUS ICES AS A FUNCTION OF ICE TEMPERATURE[a]

Temperature (K)	CO on CO Time (yr)	CO on H_2O Time (yr)	CO_2 on CO_2 Time (yr)	CO_2 on H_2O Time (yr)	H_2O on H_2O Time (yr)
10.....	8×10^{21}	6×10^{55}	7×10^{96}	2×10^{104}	2×10^{179}
20.....	1×10^{1}	1×10^{18}	3×10^{38}	1×10^{42}	6×10^{84}
30.....	1×10^{-6}	2×10^{5}	9×10^{18}	3×10^{21}	8×10^{49}
40.....	3×10^{-9}	1×10^{-1}	2×10^{9}	1×10^{11}	3×10^{32}
50.....	...	2×10^{-5}	3×10^{3}	7×10^{4}	1×10^{22}
60.....	...	6×10^{-8}	3×10^{-1}	5×10^{0}	1×10^{15}
70.....	...	1×10^{-9}	5×10^{-4}	6×10^{-3}	1×10^{10}
80.....	...	...	4×10^{-6}	4×10^{-5}	2×10^{6}
90.....	...	...	1×10^{-7}	7×10^{-7}	3×10^{3}
100.....	...	...	5×10^{-9}	3×10^{-8}	1×10^{1}
110.....	...	...	...	2×10^{-9}	2×10^{-1}
130.....	...	...	...	...	2×10^{-4}
150.....	...	...	...	...	1×10^{-6}

[a] Residence time calculated using $t = \nu_0^{-1} \exp(\Delta H_s/kT)$.

TABLE 5B

VALUES USED FOR $(\Delta H_s/k)$

System	$(\Delta H_s/k)$	Reference
CO on CO	960 K	Sandford and Allamandola 1988
CO on H_2O	1740 K	This paper
CO_2 on CO_2	2690 K	This paper
CO_2 on H_2O	2860 K	This paper
H_2O on H_2O (amorphous)	4815 K	Sandford and Allamandola 1988

The difference in behavior between CO and CO_2 trapped in H_2O is not simply due to differences in dispersive binding forces, but it suggests that CO_2 molecules are too large (covalent site size of $5.3 \times 3.0 \times 3.0$ Å) to migrate through the H_2O lattice, whereas the smaller CO molecules ($4.6 \times 3.4 \times 3.5$ Å) can.

The situation is very different, however, in ices with higher CO_2 concentrations. In the $H_2O:CO_2 = 5:1$ ice, CO_2 loss commences at 85 K, the temperature at which pure CO_2 begins to sublime. Approximately 20% of the CO_2 leaves as the ice is warmed from 85 to 100 K and another 20% is lost during warm-up to 150 K. Unlike the $H_2O:CO_2 = 20:1$ ices, the final loss of CO_2 from the 5:1 ice is *not* coupled to the sublimation of the H_2O lattice. Instead, once heated to 150 K, the CO_2 escapes the ice within 20 minutes, leaving behind a relatively pure H_2O ice which subsequently sublimes away at a slower rate. This behavior is qualitatively similar to the results of Hudson and Donn (1988) for 2:1 ices.

The $H_2O:CO_2 = 1:1$ ice shows even more extreme behavior. While it too does not lose appreciable CO_2 below 85 K, essentially *all* the original CO_2 is lost between 85 K and 100 K. At 100 K, the only remaining material is an ice containing the original H_2O with a residual amount of CO_2 in a 90 to 1 ratio. This behavior is similar to that reported by Bar-Nun *et al.* (1985) for $H_2O:CO_2 = 1:3$ ices in which most of the CO_2 was released between 80 and 130 K. These data suggest that once CO_2 is present at about the 20% level or higher, the CO_2 prevents the H_2O from forming a completely coherent hydrogen-bonded lattice. The result is an ice structure with interconnecting molecular "pores." Since the binding energy of CO_2 to H_2O is about the same as CO_2 to CO_2, the CO_2 in this porous structure becomes free to move through the ice as soon as its temperature rises above the CO_2 sublimation point.

In summary, CO_2 loss from H_2O ices having less than 5% CO_2 is entirely controlled by the H_2O. The CO_2 is physically trapped in the H_2O lattice. However, at concentrations of 20% or greater, CO_2 prevents the H_2O from forming a complete lattice and actually mediates the molecular structure of the H_2O ice lattice. In this case, the CO_2 is free to leave the resulting "porous" ice at temperatures above about 85 K.

v) *The Influence of Entrapped* CO_2 *on* H_2O *Vaporization*

The presence of 5% CO in H_2O ices has been shown to produce a 5% loss in H_2O during warm-ups below the sublimation point of pure H_2O (Sandford and Allamandola 1988). In order to test whether CO_2 produces a similar effect, the strengths of the 3290 and 1660 cm^{-1} H_2O bands were monitored in pure H_2O and $H_2O:CO_2 = 50$, 20, 5, and 1 ices as they were warmed at 2 K per minute. In contrast to CO, the presence of CO_2 in H_2O ices did not produce any additional H_2O loss during warm-up to 150 K, even for the $H_2O:CO_2 = 1:1$ ice. Thus, the presence of CO_2 does not seem to alter the effective volatility of H_2O ices.

IV. ASTROPHYSICAL APPLICATIONS

Much of the theoretical work on astrophysical ices proceeds with the assumption that the physical and thermodynamic properties of pure components provide a reasonable approximation for their behavior in mixed ices. These results demonstrate, once again, that this is incorrect and can lead to erroneous conclusions since interactions between different species in the ice can dramatically alter these properties. The

results reported here have important implications for a number of interstellar and cometary applications.

a) *Observational Requirements and Potential*

Astronomical infrared spectroscopic measurements of the solid-state CO_2 bands can be used to derive CO_2 column densities and abundances, determine the fraction of cosmic C and O in this molecule, and place important constraints on the thermal history and chemical environment of the CO_2-containing ices. However, the spectral variations expected for interstellar CO_2 are relatively small, and observations with high (by current astronomical standards) spectral resolution ($\lambda/\Delta\lambda \sim 2000$) are required to extract this information. High resolution is also needed to help disentangle the ro-vibrational lines of any gas phase CO_2 that may be along the line of sight. Moreover, since the expected variations in spectroscopic details of many of the solid-state CO_2 features are generally small, high signal-to-noise (~ 100) studies are imperative. High signal-to-noise spectra will also be required if $^{13}C/^{12}C$ ratios are to be determined using the relative strengths of the $^{12}CO_2$ and $^{13}CO_2$ bands near 2340 and 2280 cm^{-1}, respectively.

b) CO_2 *in Interstellar Clouds*

Theoretical interstellar grain mantle compositions which consider CO_2 have been calculated using models that employ both gas phase and grain surface reactions (Tielens and Hagan 1982; d'Hendecourt, Allamandola, and Greenberg 1985). Three distinct chemical regimes, each driven by the composition of the gas phase, are predicted from these calculations (see Tielens and Allamandola 1987). First, when atomic hydrogen is more abundant in the gas phase than the heavier species (e.g., CO, O, and O_2), the calculated grain mantle will be dominated by polar, hydrogenated species such as H_2O, H_2CO, and possibly CH_3OH, with CO_2 only a trace constituent. Second, when atomic hydrogen is less abundant than the heavier species and most of the oxygen is in molecular form, few reactions will occur, and the grain mantle will reflect the gas phase composition. In this case, CO, O_2, and possibly CO_2 become important grain mantle species. Third, when atomic hydrogen is less abundant than the heavier species and atomic oxygen is present, the grain mantles should be rich in less polar, oxygenated species such as CO, O_2, O_3, and CO_2. While the grain surface reaction to produce CO_2 from CO and O may be inhibited at low temperatures (Grim and d'Hendecourt 1986), irradiation of these ices certainly produces CO_2 (Moore *et al.* 1983; Allamandola, Sandford, and Valero 1988).

Since the detection of both broad and narrow solid-state CO infrared absorption bands in interstellar clouds shows that CO is frozen into both polar and nonpolar ices (Sandford *et al.* 1988), CO_2 will probably be similarly distributed. Thus, the solid-state CO_2 features, once detected, will probably be comprised of a broad component due to CO_2 in H_2O-rich ices and a narrower component attributable to CO_2 in H_2O-poor ices.

c) CO_2 *in Comets*

i) *The Source of Cometary* CO_2

CO_2 was detected in comet Halley by a variety of techniques (Combes *et al.* 1986; Krankowsky *et al.* 1986; Feldman *et al.* 1986). The abundance of CO_2 relative to H_2O was inferred from these data to fall between 1% and 3.5%, although it has been suggested that the CO_2 abundance may be higher during outbursts. There are several possible sources of cometary CO_2. First, molecular CO_2 could have been produced during an interstellar or protostellar phase prior to ice formation and subsequently incorporated into a comet or precometary ice grains by condensation. Second, CO_2 may have formed within precometary ice grains or in the coma via *in situ* photochemical reactions.

Since the abundance of interstellar CO_2 has not yet been measured, estimates of the interstellar, precometary CO_2/H_2O ice ratio must rely on theoretical models. Published models of the gas phase chemistry in interstellar clouds which exclude grain surface chemistry yield steady state values of CO_2/CO that lie between 1.5×10^{-2} and 5×10^{-5}, depending on the assumed cloud conditions (Iglesias 1977; Prasad and Huntress 1980). In models which include both grain surface reactions and gas phase chemistry, CO_2 can dominate CO if the controversial reaction CO + O is possible on grain surfaces at low temperatures (Tielens and Hagen 1982; d'Hendecourt, Allamandola, and Greenberg 1985; Grim and d'Hendecourt 1986).

In addition to the direct condensation of CO_2, it is possible that CO_2 was formed within the ice by radiation. Irradiation of the ice could have occurred either on the surface of the comet or in the interstellar/precometary phase. Cosmic-ray effects will dominate radiation-induced processes once the comet has formed since they can penetrate about 10 m into the ice, while ultraviolet radiation can only penetrate the first 1000 Å. Although cosmic rays readily form CO_2 within ices (Moore *et al.* 1983, and references therein), they are unable to produce CO_2 throughout the entire comet. CO_2 was observed from comet Halley during its 1986 apparition. This comet, with a period of about 76 yr, has made many orbits around the Sun and lost many tens of meters from its original surface. Since the time required to substantially alter the top few meters of a comet by cosmic rays is on the order of 10^9 yr (see Moore *et al.* 1983; Johnson, Cooper, and Lanzerotti 1986), there is not enough time between perihelion passages to explain the CO_2 abundances seen in comet Halley in terms of cosmic-ray production. We conclude therefore that cosmic rays are not the major contributor to the production of cometary CO_2.

Despite its insignificant role in the alteration of the interiors of comets, ultraviolet radiation *is* important during the precometary phase. CO_2 produced within interstellar ices may be incorporated in the comet during accretion. The photolysis of any ice mixture containing a source of carbon and H_2O invariably results in the production of CO_2 (see Hagen, Allamandola, and Greenberg 1979; d'Hendecourt *et al.* 1986; Sandford *et al.* 1988). The quantum efficiency for the conversion of CO into CO_2 via *in situ* ultraviolet photolysis in simple binary H_2O:CO (20:1) ices is on the order of a few percent (Sandford *et al.* 1988). From other experiments, it is known that the presence of other molecules tends to screen out the ultraviolet photons and the efficiency usually drops (Allamandola, Sandford, and Valero 1988).

Adopting a quantum efficiency of 1%, we find that a precometary ice CO_2/H_2O value of 3% is consistent with an ultraviolet fluence in the photolytically important region below 2000 Å of about 10^{19} photons cm^{-2} for an optically thin ice. This is a relatively modest exposure. The ultraviolet flux in the diffuse interstellar medium is approximately 10^8 photons cm^{-2} s^{-1}. The flux within dense molecular clouds is less than this and depends on the optical depth of the cloud. At least a tenth of the photons will penetrate to optical depths of 3, a thousandth will penetrate to optical depths of 10, and only a millionth will penetrate to an optical depth of 20 (Hagen,

Allamandola, and Greenberg 1979). Thus, the ultraviolet fluence required to produce the observed CO_2 could be accumulated in the interstellar cloud phase in as little as 10^4 to 5×10^6 yr, provided the optical depth of the cloud is less than 10. For clouds with larger optical depths, internal sources of radiation produce an ultraviolet flux between 10^{-5} and 10^{-4} that of the diffuse interstellar field (Norman and Silk 1980; Prasad and Tarafdar 1983). Consequently, sufficient photoprocessing can occur in dense clouds on time scales of 10^6–10^8 yr, a period comparable to the lifetime of most molecular clouds (Elmegreen 1985). Ultraviolet exposure could also have occurred during an active protosolar or T Tauri phase of the Sun. Thus, substantial amounts of CO_2 could have been produced in the ice phase via ultraviolet photolysis prior to cometary formation.

Finally, the possibility that CO_2 is produced by solar irradiation of ice grains ejected into the coma must also be considered. The solar ultraviolet flux at 1 AU is about 10^{13} photons cm^{-2} s^{-1}. With this flux, an optically thin ice grain must be exposed for about 20 days to produce the required amount of CO_2. This is much longer than the evaporative time scale for an optically thin ice grain at 1 AU. Therefore, the observed CO_2 is not produced in the ice particles after cometary ejection.

We conclude that the CO_2 that exists in cometary ices probably has an interstellar/precometary origin. While the CO_2 may include molecules accreted directly from the gas phase, the above arguments suggest that much of the CO_2 must have been produced within precometary ice grains by photolysis.

ii) *Cometary Activity*

1. *Activity in "normal" comets.*—H_2O is thought to control the surface temperature and vaporization behavior of the majority of cometary nuclei (Delsemme 1982, 1983; Spinrad 1987; Schmitt and Klinger 1987, and references therein). This is expected to be true independent of whether the H_2O ice is in its amorphous or cubic form (Klinger 1981; Smoluchowski 1981*a*, *b*; Herman and Weissman 1987; Prialnik and Bar-Nun 1987; Prialnik, Bar-Nun, and Podolak 1987).

The presence of smaller amounts of more volatile components, however, can alter this behavior. For instance, the presence of CO in H_2O ices produces new effects not found in pure H_2O ices (Bar-Nun *et al.* 1987; Sandford and Allamandola 1988), including CO loss with minor H_2O loss enhancement below the normal H_2O sublimation temperature. The experiments reported here show that, while the presence of CO_2 in H_2O ices affects the structure of the H_2O, CO_2 does *not* act like a lower volatility analog of CO.

For the H_2O to CO_2 ratio of about 30 observed in Halley, CO_2 is not expected to have any major effect on the vaporization behavior of the comet. At these concentrations, CO_2 does not enhance H_2O loss, and very little CO_2 can leave prior to the sublimation of the H_2O ice lattice. The only potentially observable effect would be the minor losss of CO_2 during the amorphous-to-crystalline H_2O ice transition.

Thus, it is clear that for CO_2 concentrations below 5%, homogeneous cometary ice theories that assume H_2O controls the vaporization behavior are valid. This is essentially the same conclusion reached for H_2O:CO ices.

2. *Cometary outbursts and activity at large heliocentric distances.*—Despite the predominance of H_2O in most comets, components more volatile than H_2O, such as CO and CO_2, appear to control sublimation rates in a few comets (Feldman 1978; A'Hearn and Cowan 1980; Houpis and Mendis 1981). Examples include comets Morehouse 1908 III, Humason 1962 VIII, Kohoutek 1973 XII, and West 1976 VI. Coma formation in these comets was similar to that of comets controlled by H_2O, except that it occurred at larger heliocentric distances (Delsemme 1982, 1983). Experiments that address the effects of CO in cometary ices are described elsewhere (Sandford and Allamandola 1988). In this section, the effects of CO_2 are considered.

In H_2O-rich ices ($H_2O/CO_2 > 20$), H_2O controls the vaporization since it forms strong, H-bonded networks and CO_2 cannot effectively migrate through this structure. CO_2 should begin to influence the vaporization behavior when its concentration is large enough to prevent the H_2O molecules from forming a complete H-bonded network. The work reported here, and previous infrared studies (Hagen, Tielens, and Greenberg 1983), have shown that the three-dimensional H-bonded network of amorphous H_2O ice begins to break down once the concentration of non–H-bonding impurities exceeds about 20%–30%. Beyond this point, the H-bonding is incomplete and the ice becomes progressively more influenced by the impurities. This implies that comets whose activity appears to be controlled by species more volatile than H_2O must contain impurities in excess of 20%–30% in some regions. For comparison, the largest amount of impurities a traditional clathrate can contain before disruption is about 15% (see Davidson *et al.* 1987, and references therein). Clathrates are much more organized than the amorphous ices produced at low temperatures and pressures.

There are indications that even in comets thought to be dominated by H_2O, more volatile components can drive cometary outbursts (Beyer 1962; Delsemme 1982; Wyckoff 1982). These outbursts may be due to explosive gas release from pockets of material rich in molecules like CO and CO_2 (Whipple 1980; Feldman *et al.* 1986). These pockets could be due to heterogeneities trapped within the nucleus during accretion (a possibility somewhat at odds with observations that suggest that cometary nuclei are largely homogeneous [Donn and Rahe 1982]) or to localized volatile enrichment by diffusional processes.

The work presented here demonstrates that such pockets cannot form via CO_2 diffusion if the initial ice has a H_2O to CO_2 ratio of 20 or greater. At concentrations of 20% or higher, however, the CO_2 forces the ice to have a "porous" structure from which the CO_2 can escape above 85 K. This escaping CO_2 can then either leave the comet (potentially producing some cometary activity at large heliocentric distances) or recondense at some colder location within the cometary nucleus. These recondensation sites could ultimately become local areas with very high CO_2 concentrations. The sudden release of gas from these pockets, triggered by sublimation of the surrounding nonporous ice or by macroscopic displacements within the nucleus, might then produce outburst activity. The consequences of such behavior within a clathrate framework are considered by Smoluchowski (1985).

Finally, we note that the presence of more than 20% CO_2 may have profound effects on the behavior of other volatiles within cometary nuclei. Once the CO_2 has evacuated the ice around 85 K, the "pores" become available for use by any other volatile present.

V. SUMMARY

The infrared spectral properties of CO_2 frozen in a number of cometary and interstellar ice analogs at different temperatures have been investigated. Detailed examination of the five infrared CO_2 bands shows that the peak position, FWHM, and profile of the bands provide important information about the composition, formation, and subsequent thermal history of the ices. Absorption coefficients of all the bands are provided for CO_2 in pure CO_2 and H_2O- and CO-rich ices. These can be used to determine interstellar CO_2 column densities and abundances. Furthermore, observations of the relative strengths of the $^{13}CO_2$ and $^{12}CO_2$ asymmetric stretch bands near 2340 and 2280 cm^{-1}, respectively, can provide information on the $^{13}C/^{12}C$ ratio in astrophysical ices. Comparison of this ratio with that found from CO will give insight into the chemistry involving these two important C-containing species. Since telluric CO_2 obscures all the CO_2 bands. this work awaits the advent of the Infrared Space Observatory and SIRTF.

Properties associated with the condensation and vaporization behavior of CO_2 and H_2O:CO_2 ices have also been determined using infrared spectroscopic techniques. The CO_2-CO_2 surface binding energy in pure CO_2 ice was found to be $(\Delta H_s/k) = 2690 \pm 50$ K. The binding energies of CO_2 and CO on H_2O ices were determined from the temperature dependence of the CO_2 and CO sticking efficiencies and were found to be approximately $(\Delta H_s/k) = 2860$ K and 1740 K, respectively. These values are expected to be valid at temperatures near the sublimation points of CO_2 and CO at low pressures.

Under the experimental conditions used, it was found that measurable amounts of CO_2 can condense out of the gas phase onto H_2O ices at temperatures as high as 100 K. This is only a modest increase over the condensation temperature of CO_2 onto pure CO_2 ices under the same conditions. The loss of CO_2 from H_2O-rich ices was found to be concentration dependent. For ices having $H_2O/CO_2 > 20$, the CO_2 is physically trapped in the H_2O lattice and remains in the solid up to temperatures of about 150 K. At this temperature, minor amounts of CO_2 (<20%) are lost during the amorphous-to-crystalline phase transition of the H_2O lattice, but most of the CO_2 leaves only when the H_2O ice itself begins to sublime. CO_2 has a profound influence on the ice for samples having $H_2O/CO_2 < 5$. At these concentrations, the CO_2 prevents the H_2O from forming a completely H-bonded network, resulting in a molecularly "porous" structure from which the CO_2 (and presumably other volatiles) can freely escape above 85 K. However, the presence of even these large amounts of CO_2 has little significant effect on the sublimation of the H_2O itself.

These results are applicable to the study of comets. In H_2O-rich ices ($H_2O > 95\%$), H_2O controls the sublimation regardless of the volatility of other components. In H_2O ices containing $CO_2 > 20\%$, the H_2O lattice is altered, and comets having such large CO_2 concentrations would be expected to relase their CO_2 at larger heliocentric distances. This process may also result in the accumulation of volatile-rich gas "pockets" within the nucleus. Gas release from these pockets could then be triggered by sublimation or physical destruction of the pocket walls and result in jetting or outburst activity.

The amount of CO_2 inferred to be present in comet Halley appears to be best explained in terms of photoproduction in the ice grain phase prior to cometary formation. Adequate ultraviolet radiation could have been supplied either during a precometary/interstellar phase or possibly during the protosolar phase.

We gratefully acknowledge support from NASA grant 19952120400.

REFERENCES

A'Hearn, M. F., and Cowan, J. J. 1980, *Moon and Planets*, **22**, 41.
Allamandola, L. J., Lucas, D., and Pimentel, G. C. 1978, *Rev. Sci. Instr.*, **49**, 913.
Allamandola, L. J., and Sandford, S. A. 1988, in *Dust in the Universe*, ed. M. E. Bailey and D. A. Williams (Cambridge: Cambridge University Press), p. 229.
Allamandola, L. J., Sandford, S. A., and Valero, G. J. 1988, *Icarus*, **76**, 225.
Anderson, A., and Walmsley, S. H. 1964, *Molec. Phys.*, **7**, 583.
Bar-Nun, A., Dror, J., Kochavi, E., and Laufer, D. 1987, *Phys. Rev. B*, **35**, 2427.
Bar-Nun, A., Herman, G., Laufer, D., and Rappaport, M. L. 1985, *Icarus*, **63**, 317.
Barrett, C. S., and Meyer, L. 1965, *J. Chem. Phys.*, **43**, 3502.
Beyer, M. 1962, *Astr. Nach.*, **286**, 219.
Cahill, J. E., and Leroi, G. E. 1969, *J. Chem. Phys.*, **51**, 1324.
Combes, M., *et al.* 1986, *Nature*, **321**, 266.
———. 1988, *Icarus*, **76**, 404.
d'Hendecourt, L. B., and Allamandola, L. J. 1986, *Astr. Ap. Suppl.*, **64**, 453.
d'Hendecourt, L. B., Allamandola, L. J., and Greenberg, J. M. 1985, *Astr. Ap.*, **152**, 130.
d'Hendecourt, L. B., Allamandola, L. J., Grim, R. J. A., and Greenberg, J. M. 1986, *Astr. Ap.*, **158**, 119.
d'Hendecourt, L. B., and Jourdain de Muizon, M. 1989, *Astr. Ap.*, **223**, L5.
Davidson, D. W., Desando, M. A., Gough, S. R., Handa, Y. P., Ratcliffe, C. I., Ripmeester, J. A., and Tse, J. S. 1987, *Nature*, **328**, 418.
Delsemme, A. H. 1982, in *Comets*, ed. L. L. Wilkening (Tucson: University of Arizona Press), p. 85.
———. 1983. *J. Phys. Chem.*, **87**, 4214.
Donn, B., and Rahe, J. 1982, in *Comets*, ed. L. L. Wilkening (Tucson: University of Arizona Press), p. 203.
Elmgreen, B. G. 1985, in *Protostars and Planets II*, ed. D. C. Black and M. S. Matthews (Tucson: University of Arizona Press), p. 33.
Falk, M. 1987, *J. Chem. Phys.*, **86**, 560.
Falk, M., and Seto, P. F. 1986, *Canadian J. Spectrosc.*, **31**, 134.
Feldman, P. D. 1978, *Astr. Ap.*, **70**, 547.
Feldman, P. D., A'Hearn, M. F., Festou, M. C., McFadden, L. A., Weaver, H. A., and Woods, T. N. 1986, *Nature*, **324**, 433.
Fredin, L., Nelander, B., and Ribbegard, G. 1974, *J. Molec. Spectrosc.*, **53**, 410.
Frenkel, Z. 1924, *Zs. Phys.*, **26**, 117.
Greenberg, J. M. 1982, in *Comets*, ed. L. L. Wilkening (Tucson: University of Arizona Press), p. 131.
Grim, R. J. A., and d'Hendecourt, L. B. 1986, *Astr. Ap.*, **167**, 161.
Guasti, R., Schettino, V., and Brigot, N. 1978, *Chem. Phys.*, **34**, 391.
Hagen, W., Allamandola, L. J., and Greenberg, J. M. 1979, *Ap. Space Sci.*, **65**, 215.
Hagen, W., Tielens, A. G. G. M., and Greenberg, J. M. 1983, *Astr. Ap. Suppl.*, **51**, 389.
Herman, G., and Weissman, P. R. 1987, *Icarus*, **69**, 314.
Hobbs, P. V. 1974, *Ice Physics* (Oxford: Clarendon Press).
Houpis, H. L. F., and Mendis, D. A. 1981, *Moon and Planets*, **25**, 95.
Hudson, R. L., and Donn, B. 1988, *Icarus*, submitted.
Iglesias, E. 1977, *Ap. J.*, **218**, 697.
Irvine, M. J., Mathieson, J. G., and Pullin, D. E. 1982*a*, *Australian J. Chem.*, **35**, 1961.
———. 1982*b*, *Australian J. Chem.*, **35**, 1971.
Johnson, R. E., Cooper, J. F., and Lanzerotti, L. J. 1986, in *Proc. 20th ESLAB Symposium on Exploration of Halley's Comet*, ed. B. Battrick, E. J. Rolfe, and R. Reinhard (ESA SP-250), p. 269.
Klinger, J. 1981, *Icarus*, **47**, 320.
Krankowsky, D., *et al.* 1986, *Nature*, **321**, 326.
Langescheidt, E., Patnaik, A., and Roessler, K. 1990, in *Proc. 61st International School of Physics*, "*Enrico Fermi*," ed. E. Bussoletti and G. Strazzulla (Amsterdam: North Holland), in press.
Langmuir, I. 1916, *Phys. Rev.*, **8**, 149.
Laufer, D., Kochavi, E., and Bar-Nun, A. 1987, *Phys. Rev. B*, **36**, 9219.
Leighton, R. B., and Murray, B. C. 1966, *Science*, **153**, 136.
Moore, M. H., Donn, B., Khanna, R., and A'Hearn, M. F. 1983, *Icarus*, **54**, 388.
Norman, C., and Silk, J. 1980, *Ap. J.*, **238**, 158.
Osberg, W. E., and Hornig, D. F. 1952, *J. Chem. Phys.*, **20**, 1345.
Prasad, S. S., and Huntress, W. T., Jr. 1980, *Ap. J.*, **239**, 151.
Prasad, S. S., and Tarafdar, S. P. 1983, *Ap. J.*, **267**, 603.
Prialnik, D., and Bar-Nun, A. 1987, *Ap. J.*, **313**, 893.
Prialnik, D., Bar-Nun, A., and Podolak, M. 1987, *Ap. J.*, **319**, 993.
Ron, A., and Schnepp, O. 1967, *J. Chem. Phys.*, **46**, 3991.

Sandford, S. A., and Allamandola, L. J. 1988, *Icarus*, **76**, 201.
Sandford, S. A., Allamandola, L. J., Tielens, A. G. G. M., and Valero, G. J. 1988, *Ap. J.*, **329**, 498.
Schmitt, B., and Klinger, J. 1987, in *Symposium on the Diversity and Similarity of Comets*, ed. E. J. Rolfe and B. Battrick (ESA SP-278), 613.
Smith, A. W. 1929, in *International Critical Tables, Vol. 5*, ed. E. Washburn (New York: McGraw-Hill), p. 138.
Smoluchowski, R. 1981*a*, *Ap. J.* (*Letters*), **244**, 31.
———. 1981*b*, *Icarus*, **47**, 312.
———. 1985, in *Ices in the Solar System*, ed. J. Klinger, D. Benest, A. Dollfus, and R. Smoluchowski (Dordrecht: Reidel), p. 397.
Spinrad, H. 1987, *Ann. Rev. Astr. Ap.*, **25**, 231.
Tielens, A. G. G. M., and Allamandola, L. J. 1987, in *Interstellar Processes*, ed. D. Hollenbach and H. Thronson (Dordrecht: Reidel), p. 397.
Tielens, A. G. G. M., and Hagen, W. 1982, *Astr. Ap.*, **114**, 245.
Tso, T., and Lee, E. K. C. 1985*a*, *J. Phys. Chem.*, **89**, 1612.
———. 1985*b*, *J. Phys. Chem.*, **89**, 1618.
Warren, S. G. 1986, *Appl. Optics*, **25**, 2650.
Whipple, F. L. 1980, *A.J.*, **85**, 305.
Wood, B. E., and Roux, J. A. 1982, *J. Opt. Soc. Am.*, **72**, 720.
Wyckoff, S. 1982, in *Comets*, ed. L. L. Wilkening (Tucson: University of Arizona Press), p. 3.
Yamada, H., and Person, W. B. 1964, *J. Chem. Phys.*, **41**, 2478.

LOUIS J. ALLAMANDOLA and SCOTT A. SANDFORD: NASA/Ames Research Center, Mail Stop 245-6, Moffett Field, CA 94035